Compact UHF RFID Balun-Like Integrated Tag Antenna for Long Range Detection of Water Bottles

Manoj Garg[1], Ashwani Sharma[1], Ignacio J. Garcia Zuazola[2] (Member IET), Arjit Gupta[1]*

[1] *Electrical Engineering Department, Indian Institute of Technology Ropar, Punjab, 140001, India.*
[2] *School of Computing and Digital Media, London Metropolitan University, London N7 8DB, UK*
* *E-mail: i.garciazuazola@londonmet.ac.uk*

Abstract: A compact, flexible, long-range, and impedance transformer balun-like integrated UHF RFID tag antenna is proposed for the detection of water bottles. To alleviate the performance of a tag antenna in close proximity to a high dielectric material such as water, the radiating element of the tag antenna uses folded, unbalanced strips made of balun-like arms wrapped around the tag's body. As a result, a wide bandwidth with reasonably good radiation resistance is achieved. The tag's body comprises dual-loops for the impedance matching to the tag chip. This leads to a long read range of 13.33 m; > 5.83 m compared to other state-of-the-art designs. The proposed tag antenna conforms to a small footprint by wrapping the balun-like arms around the tag's body, which results in a compact form. The tag is fabricated, and the results reasonably agree with simulations.

1 Introduction

Radio-Frequency Identification (RFID) is perceived as an integral technology for applications such as the Internet of Things (IoT) [1], management of goods and objects [2], healthcare [3], animal tracking [4], electronic toll collection, asset identification, etc. RFID readers use back-scattering to retrieve the tag's unique identification. The operating frequency band for the UHF RFID is allocated between 840 MHz to 960 MHz worldwide, specifically $865 - 868$ MHz for Europe, New Zealand, and India, $902 - 928$ MHz for the USA, $940 - 943$ MHz for China, and $908.5 - 914$ MHz for Korea [5, 6]. Due to its widespread applications, several cost-effective, small, and malleable solutions exist for RFID tags. However, their performance is inherently compromised when attached to water bottles, as a result, the reading range decreases due to low gain and impedance mismatch with the tag chip [7]. Therefore, particularly for applications such as liquid inventory, the design process of the tags must take into account the permittivity of water [8]. Moreover, a compact, long-range and flexible tag is preferred to easily attach to naturally curved bottles. This is performed using an efficient conjugate impedance matching technique to match the tag antenna impedance with the RFID chip.

In the literature, several design techniques were reported to improve the tag performance on water bottles. For instance, a T-matching technique was used in [7, 11–17] to monitor the tag on wine and water bottles. Similarly, a few designs for water leveling and distance monitoring were proposed in [18, 19], having limited read range with large dimensions. However, the T-matching technique did not provide wide bandwidths. Therefore, to achieve better impedance matching on the liquid-filled bottles, two loops are used. For instance, some tag antenna incorporating a nested slot feed was proposed in [8, 20, 21, 23, 25–31] to improve impedance matching, however, offering a read range of ~ 2.5 m. The nested slot technique showed large dimensions [22], with adverse effects in close proximity of water. Similarly, a conformal tag antenna with a reading range of 3.5 m [32, 41] was proposed for a smart blood repository system to track blood bags [33]. Furthermore, RFID tags were proposed for liquids such as intravenous (IV) [34, 35], shakes, wine, and orange juice [36]. Similarly, a slot enabled near body tag was proposed in [37]. The aforementioned designs have relatively large dimensions, and a few are inflexible with a low read range. Moreover, the water bottle industry employs stacked or piled packing, therefore, mutual coupling occurs between tags, resulting in

compromised gain and impedance mismatching. Thus, water bottle monitoring and identification is an issue in dynamic and different environments within industry. Moreover, a bidirectional tag antenna was proposed in [38] to reduce the mutual coupling between tags.

Thus, to satisfy the current needs of tag antennas with low footprint but long read range detection of water bottles, a compact, flexible, mutual coupling insensitive UHF RFID Balun-Like Integrated Tag Antenna for Long Range Detection of Water Bottles is proposed. This paper comprises six sections. Introduction was reported in Section 1. The problem analysis of conventional designs with the proposed design is presented in Section 2, the simulated results including a parametric study in Section 3, and the fabrication and measurements in Section 4. The paper is concluded in Section 5.

2 Proposed System Model

The schematic model of the proposed UHF RFID tag antenna for tracking water-filled bottles in commercial industry applications is shown in Fig. 1. Each carton box in the warehouses is filled with M
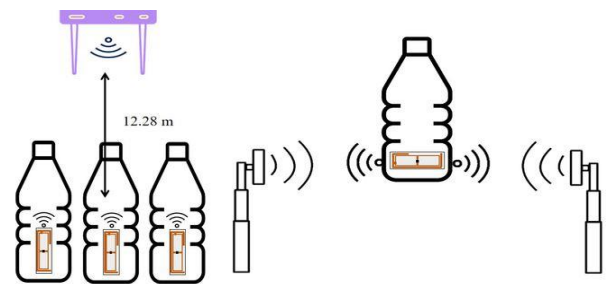
Fig. 1: Schematic model of the proposed UHF RFID tag for water bottle applications in industry.

$\times$ N closely packed water bottles, and each bottle is labeled with an RFID tag. Therefore, a bore-sight radiation pattern is not desired for this specific application as the bore-sight affects the tag performance negatively due to mutual coupling with unlikely read tags. Hence, a bi-directional antenna is required to overcome the mentioned issue.

2.1 Observation and problems in conventional designs

For the evolution of the proposed design, tags with conventional impedance matching techniques were investigated and printed on a single-sided polyester substrate (a label) having $\epsilon_r = 3.2$, $\tan\delta = 0.002$, and thickness 0.1 mm with copper ink deposition of 10 microns using commercial electromagnetic software Ansys HFSS. The conventional tags were simulated over High-Density Poly Ethylene (HDPE) bottle of 1mm thickness [7] filled with water, as illustrated in Fig. 2. This assumed a dielectric constant and electrical conductivity of water (H_2O) respectively as $\epsilon_r = 81$ and $\sigma = 0.01$ S/m. Their corresponding current distributions with water are
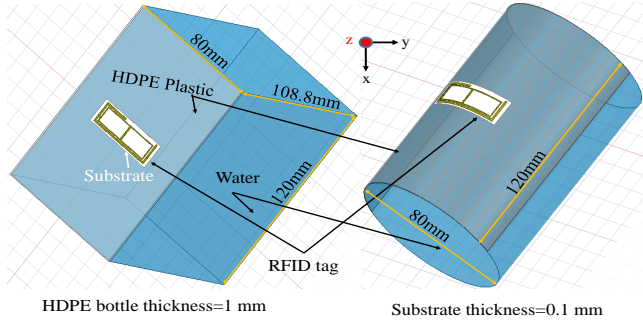
Fig. 2: Simulation layout of the proposed tag antenna (left) on a container and (right) on a water bottle.
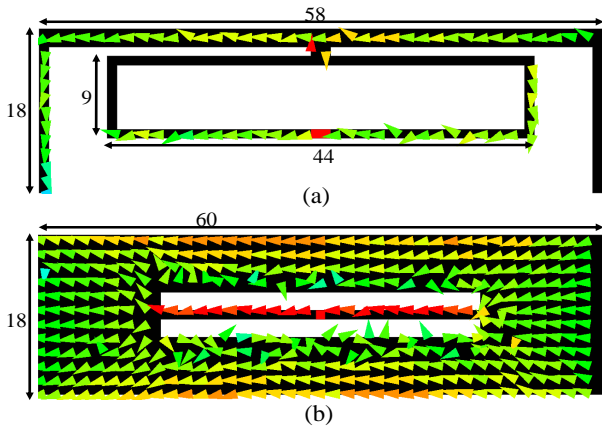
Fig. 3: Current distributions for (a) T-matching, (b) Nested H-shaped slot [39] with water bottle

.

presented in Fig. 3. The results using T-matching techniques are illustrated in Fig. 3 (a), which show non-uniform currents in the presence of water. On the other hand, the nested H-shaped slot technique of Fig. 3 (b) showed more balanced current distributions with relatively larger dimensions and low gain. To corroborate this in regard to their input reactance, the immediately outlined techniques were simulated at 866 MHz, and their corresponding impedances are presented in Table 1. It is noted that the reactance of the T-matching and

Table 1 Impedance for the Different Techniques

Techniques	With water bottle (η_r)	Gain (dBi)
T-Matching	62.17 + j237.50 (12 %)	-5.5
Nested H-shaped slot	14 + j120.57 (19 %)	-2.1

nested H-shaped slot vary significantly in the presence of water from

the chip impedance ($Z_c = 38.83 + j153.30$). In addition, similar results are obtained from conventional reported T-matching [9, 10] and nested H-shaped slot designs [8, 12, 18, 19, 21] where the reading range of the tags was constrained in the presence of water. The T-matching technique reported a limited bandwidth, and the impedance of the tag antenna varied significantly in the presence of water. Similarly, the nested slot technique has large size radiators and the radiation efficiency (η_r) of both tags was constrained in the presence of water. The following problems are observed in the conventional UHF RFID tags:

• The impedance changes significantly in the presence of water, therefore, to design an efficient tag antenna, it must be impedance tolerant.
• The efficiency is reduced in the presence of water, therefore, an efficient tag antenna is desired.

Following the immediately mentioned observations, a novel UHF RFID tag antenna is proposed, and its performance in the presence of water is discussed in the next subsection.

2.2 Design

The dimensions of the proposed tag antenna is shown in Fig. 4. The
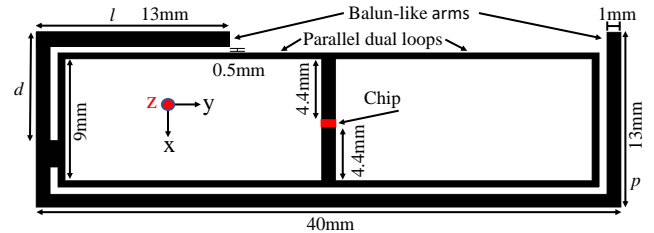
Fig. 4: Dimensions of the proposed tag antenna.

tag antenna comprises a radiating element using unbalanced strips made of balun-like arms, and these arms were wrapped around the tag's body (the parallel dual-loops) to minimize the overall size of the tag. The unbalanced strips led to an optimum design with reasonably good impedance matching, current density, and long read range. The parallel dual-loops were used for their relatively good reactive impedance matching on high permittivity (water) compared to other conventional methods; this is achieved by a widespread magnetic field (H-field) distribution in the near-field which is less affected in the presence of water. The design evolution is presented next.

2.3 Design evolution

The initial antenna element was designed using the parallel dual-loops to obtain a wider bandwidth and relatively good impedance matching on high permittivity (water) in the desired UHF RFID band, as shown in Fig. 5. The dual loops were simulated following
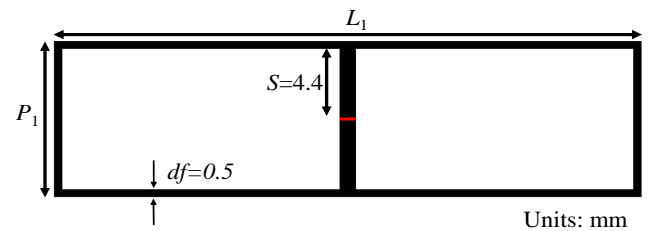
Fig. 5: Dimensions of the loop antenna.

the procedure of Fig. 2; an input impedance of (22.12 + j136.69)

is obtained. The parametric analysis for this is reported later Section 3.1. To satisfy the second condition, in which η_r is to be improved, the radiating arms (unbalanced strips) of the proposed tag antenna were targeted for compactness and, thus, carefully wrapped around the dual-loops to minimize the adverse effects of the water. This is in contradiction with conventional approaches where large-size radiators are common.

It is noted that the reactance of the T-matching and nested H-shaped slot vary significantly in the presence of water, whereas the parallel dual-loops with reactance 136.69 Ω offered relatively good conjugate matching with the chip's reactance (-154.31 Ω) when attached to the water bottle. Furthermore, the η_r of the reported designs was ~ 12 %, whereas the proposed tag antenna was 27 % in the presence of water. The folded, unbalanced strips of balun-like arms wrapped around the parallel dual-loops are presented next.

2.4   Effect of Unbalanced Strips
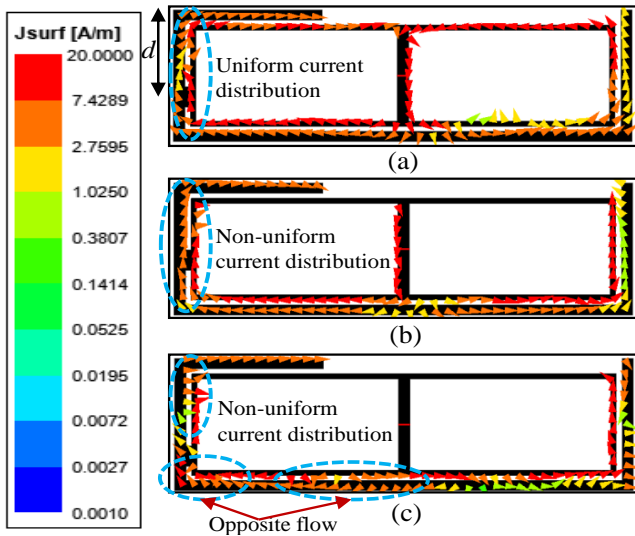
Fig. 6: Current distributions (a) with water bottle for $d = 7.6$ mm (b) $d = 6.6$ mm and (c) $d = 8.6$ mm.

The effect of the unbalanced strips was observed by evaluating the current distributions shown in Fig. 6. The differential mode/common mode (DM/CM) was defined by means of the current distribution along the tag antenna. Whereas in the dual-loops a DM was present due to the opposite currents flowing at every point in the loops, in the unbalanced strips a CM was triggered from currents flowing in an even direction. The effect with the water bottle, depicted in Fig. 6 (a), demonstrated that the currents in the unbalanced strips flowed constructively with the dual-loops. This is because the proposed tag antenna (unbalanced strips connected to parallel dual-loops) serves as an impedance transforming balun, enabling a DM current in the dual-loops and a CM in the unbalanced strips depending on design parameters. To corroborate this, the current distribution of the tag for various lengths of d (defined in Fig. 4) are shown in Fig. 6 (a-c), where d defines the location of the joint between the unbalanced strips and the dual-loops. For $d = 6.6$ mm, the current magnitude distribution in the dual-loops was non-uniform (Fig. 6 (b)), similarly, for $d = 8.6$ mm Fig. 6 (c), the DM current distribution existed in the dual loops. However, when $d = 7.6$ mm (Fig 6 (a)), desired current distributions in the dual-loops and the unbalanced strips were found, corroborating the impedance transformer balun-like behavior. The following input impedances, 38.83 $+$ j153.30, 36.44 $+$ j154.80, and 29.62 $+$ j159.76, were observed for $d = 6.6$ mm, 7.6 mm, and 8.6 mm, respectively, proving that out-of-phase currents in the unbalanced strips (balun-like arms) affected the impedance matching of the tag positively.

3   Simulated Results

The proposed tag antenna was simulated to evaluate its input impedance $Z_a = R_a + jX_a$, gain $G_r(\phi, \theta)$, and read range performance by following the procedure of Fig. 2. The read range, d, was calculated theoretically using Friss equation as

$$d = \frac{\lambda}{4\pi} \sqrt{\frac{P_t G_t(\phi, \theta) G_r(\phi, \theta) \tau P_m}{P_{th}}} \qquad (1)$$

where P_t is the transmitter power, G_t is the gain of the transmitter antenna, P_{th} is the chip sensitivity (-22.5 dBm), and P_m is the polarization mismatch efficiency ($P_m = 0.5$ for the circularly polarized transmitter antenna). Here, τ is the power transmission coefficient and can be calculated as

$$\tau = \frac{4R_c R_a}{|Z_c + Z_a|^2}, 0 \leq \tau \leq 1 \qquad (2)$$

where $Z_c = R_c - jX_c$ is the chip impedance. For the conjugate matching, a 1.13 pF capacitance with a parallel resistance of 0.7 kΩ was assumed for the chip. The impedance matching between the tag antenna and chip was estimated using (2), and the simulated input impedance of the proposed tag antenna with and without a water bottle is illustrated in Fig. 7. Since the antenna was tailored for water
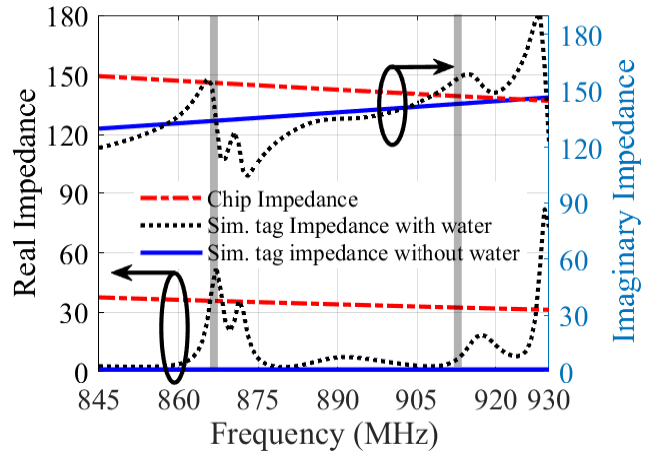
Fig. 7: Impedance of the proposed tag antenna with and without water bottle.

applications, it is observed that the impedance of the proposed tag antenna (with water) is well matched to the chip impedance in ETSI and FCC bands. However, this is not the case when the water is not present. That is a compromised 25 % efficiency.

3.1   Parametric analysis

A parametric study of the unbalanced strips was carried out by varying l and p at 866 MHz to maximize the reading range. The thickness of the water bottle was 1 mm, and the length of l and p were varied in $1 - 20$ mm and $1 - 15$ mm range, respectively. The maximum reading range of ~ 13.33 m is shown in Fig. 8 when $l = p = 13$ mm, which corresponds to a simulated gain of 0.2 dBi. Furthermore, the parametric study of the dual loops (P_1 and L_1 in Fig. 5) was conducted to analyze the effects of its dimension on the impedance matching, results are shown in Table 2. The P_1 and L_1 were chosen 10 and 37, respectively, based on the impedance matching, since other dimensions exhibit significant reactance, which fluctuates more during the integration of unbalanced strips.

3.1.1   Effect of bottle thickness:
The proposed tag antenna was attached to HDPE plastic bottles of different thicknesses ($0.3 - 1.5$mm) to investigate the impact of bottle thickness on the reading
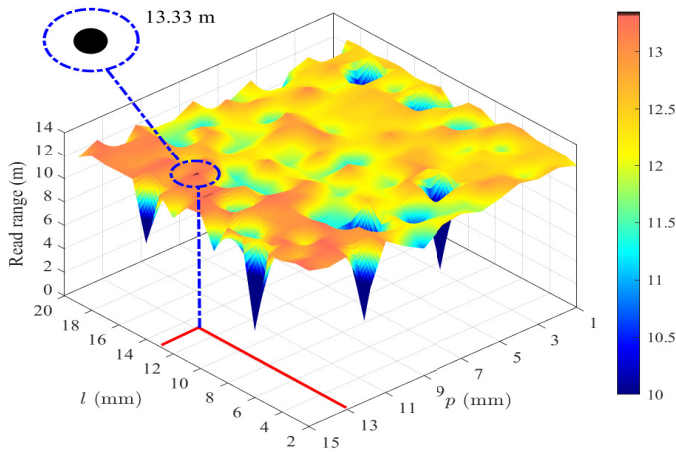
Fig. 8: Parametric study of the unbalanced strips at 866MHz for tag on water-filled HDPE bottle.

Table 2 Parametric study of dual loop impedance at 866MHz for tag on water-filled bottle.

S.N.	P_1 (mm)	L_1 (mm)	Impedance (Ω)
1.	9	36	$15.24 + j160.12$
2.	9	37	$3.34 + j123.01$
3.	9	38	$31.39 + j150.09$
4.	10	36	$24.87 + j153.26$
5.	10	37	$22.12 + j136.69$
6.	10	38	$29.31 + j160.26$
7.	11	36	$24.62 + j184.98$
8.	12	37	$43.87 + j169.47$
9.	13	38	$49.65 + j185.12$

range. The result indicates a maximum reading range of 14.30 m achieved for 1.5 mm bottle thickness and a minimum reading range of 10.19 m for 0.3 mm. This is shown in Table 3.

Table 3 Performance of the proposed tag on different thicknesses of the water bottle.

S.N.	Bottle-thickness (mm)	Impedance (Ω)	Gain (dBi)	Reading Range (m)
1.	0.3	$82.88 + j233.34$	0.2	10.19
2.	0.4	$54.80 + j183.40$	0.5	12.84
3.	0.5	$48.56 + j181.66$	0.1	12.39
4.	0.7	$45.92 + j162.7$	0.3	13.31
5.	1	$36.44 + j154.8$	0.2	13.33
6.	1.2	$46.56 + j155.52$	0.1	13.06
7.	1.5	$39.93 + j144.13$	0.9	14.30

3.1.2 Effect of bottle volume: The proposed tag antenna was also investigated for bottles of different volumes filled with water. Table 4 shows the effect for the different cases. Although a compromise performance can be observed for unrealistically small bottle volumes (3. and 4.), more prominent results are observed for realistic cases (1. and 2.).

3.1.3 Effect of different graded bottle: The proposed tag antenna performance was also evaluated for bottles made from various plastic materials HDPE, PET, PVC, Polypropylene (PP), and LDPE. Bottle thicknesses of 1mm were considered for this analysis. Table 5 shows reasonable impedance matching results on various plastic materials with only a slight variation in the reading range.

Table 4 Performance of the proposed tag antenna for various water bottle volumes.

S.N.	Volume-water-filled bottle (mm^3)	Impedance (Ω)	Gain (dBi)	Reading Range (m)
1.	$120 \times 80 \times 108.8$	$36.44 + j154.8$	0.2	13.33
2.	$200 \times 100 \times 120$	$5.71 + j145.88$	0	8.79
3.	$80 \times 50 \times 100$	$1.92 + j125.60$	-5.7	2.36
4.	$75 \times 50 \times 50$	$2.58 + j136.69$	-5.3	3.22

Table 5 Performance of the proposed tag antenna on the different grades of the water bottle.

S.N.	Material	Impedance (Ω)	Gain (dBi)	Reading Range (m)
1.	HDPE	$36.44 + j154.8$	0.2	13.33
2.	PET	$46.52 + j165.26$	0.6	13.72
3.	PVC	$38.6 + j159$	0.59	13.90
4.	Polypropylene (PP)	$33.72 + j138.91$	0.5	13.46
5.	LDPE	$36.81 + j156$	0.2	13.32

3.2 *Performance of the proposed tag antenna with frequency*

Although the proposed tag antenna was tailored for the 866MHz and 915MHz frequency bands, Table 6 shows its behavior for several frequency bands. A maximum reading range of 13.33 m is achieved in the ETSI band (866MHz) and a read range of 4.22 m in the lower FCC band (902MHz).

Table 6 Performance of the proposed tag antenna for in various frequency standards.

S.N.	Frequency MHz	Frequency allocated	Impedance (Ω)	Gain (dBi)	Reading Range (m)
1.	866	Europe/ India	$36.44 + j154.8$	0.2	13.33
2.	902	American	$1.93 + j137.86$	-1.9	4.22
3.	908.5	Korea	$2.79 + j145.30$	-1.4	5.59
4.	915	FCC/ American	$13.26 + j158.79$	0.3	11.92
5.	928	American	$41.15 + j186.06$	-2.4	9.11

3.3 *Magnetic field distribution and bending tolerance*

The magnetic field (H-field) distribution of the proposed tag antenna was also simulated and is illustrated in Fig. 9. The H-field was
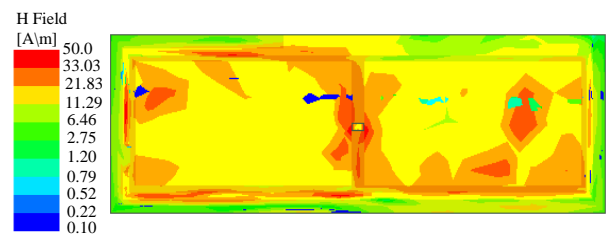
Fig. 9: H-field distribution of the proposed tag antenna.

observed in a plane 1 mm away from the tag. It is apparent from Fig. 9 that the H-field intensity is higher within the dual-loop area. It was witnessed that a large dual-loop led to wide H-field distribution and that, compared to other conventional methods, significantly improved the read range. The bending tolerance of the proposed tag antenna used as a label was evaluated when affixed on bottles of various shapes. This tag antenna was placed longitudinal or across the length of the water bottle, as shown in Fig. 10 (a). Naturally, the bending was prominent for the latter. Therefore, the read range for different bendings was simulated using the model depicted in
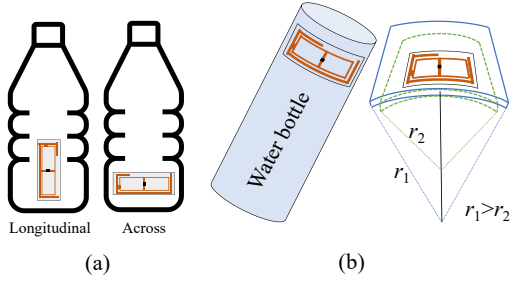
Fig. 10: The proposed tag (a) affixed on water bottle (b) bending tolerance simulation model for different bottle sizes.

Fig. 10 (b), where the bending radius is denoted as r. Note that $r = \infty$ represents a flat surface, whereas lower values of r represent a higher bending corresponding to water bottles of smaller size. The simulated read range of the proposed tag antenna on water bottles of different r is shown in Table 7. A maximum read range of

Table 7 Bending tolerance of the proposed tag on the water bottle

Radius r of bottle (mm)	∞	35	30	25	20	15
Read Range (m)	13.33	12.43	10.3	10.1	6.8	5.8

13.33 m and 5.8 m was found for $r = \infty$ and $r = 15$ mm, respectively. Additionally, results revealed that for a typical water bottle of 50 cl having $r = 35$ mm, the proposed tag antenna attained a read range of 12.43 m, which is an acceptable bending tolerance.

3.4 Mutual coupling
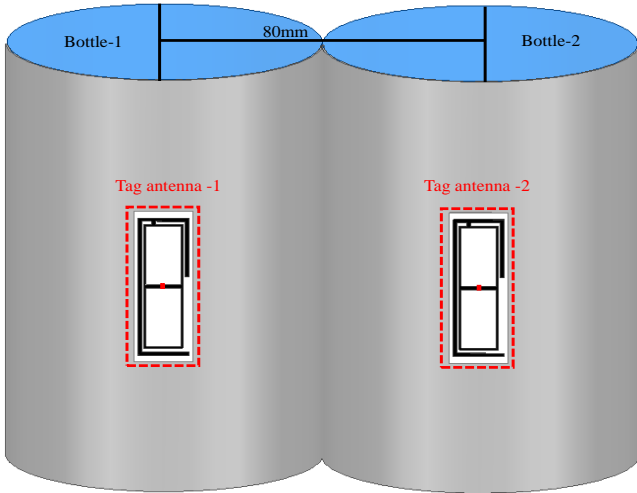
Fig. 11: Simulation of two neighboring proposed tag antennas.

Mutual coupling can cause a change in the input impedance of tag antennas, resulting in significantly reduced power transfer to the chip. Therefore, especially in systems where several RFID tag antennas must coexist, the mutual coupling should be assessed in order to validate the design. Fig. 11 shows the simulation setup, considers two neighbor models and evaluates the mutual coupling effect by stimulating both tags simultaneously. The response is given in Fig. 12 and shows a -30dB coupling effect between tags which is reasonable for stockpiling applications.
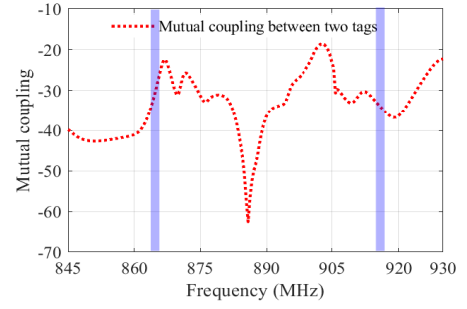
Fig. 12: Mutual coupling between two neighboring proposed tag antennas.

4   Fabrication and Measurement

The proposed tag antenna was fabricated, as shown in Fig. 13 (a), by a screen printing process, which involved a transfer of copper ink onto a single-sided polyester (typical label of a bottle of water) whose material properties were earlier detailed in Section 2.1. The
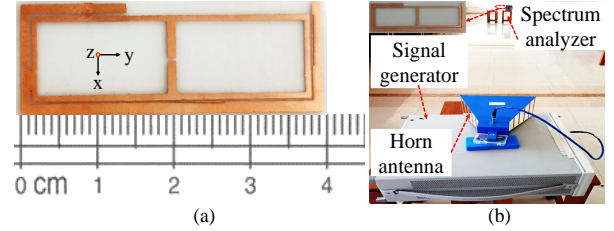
Fig. 13: (a) Fabricated and (b) measurement setup of the proposed tag antenna.

tag antenna (used as a label) was then affixed on a water bottle. The measurement setup is shown in Fig. 13 (b), which includes a 9 dBi transmitter horn antenna fed with an RF signal generator (Agilent Technologies) and a Keysight N9915A handheld spectrum analyzer (SA) connected to the proposed tag antenna for measuring received power. A matching circuit was employed for the experiments when connected to the Spectrum Analyzer (SA); the associated insertion loss (IL) was accounted for. The measurement is accurate enough since the SA is a narrow band with a lower noise floor and better dynamic range, so its sensitivity is better than traditional power meters. The signal generator was set at 27 dBm, and the received signal strength was measured using the SA. The measurements were performed for the ETSI (866 MHz) and the FCC (915 MHz) bands. It was witnessed that the proposed tag antenna had better signal strength compared to the literature. The maximum received signal strength reported in the literature is -50 dBm, compared to the proposed tag of -19 dBm; both measured 12 m away from the transmitter using the ETSI band. The proposed tag antenna was affixed to the water bottle for realistic measurements and moved carefully closer to the transmitter until a minimum of -19 dBm at 866 MHz and -20 dBm at 915 MHz was attained, which led to a read range of 12.28 m and 11.13 m for the ETSI and FCC bands respectively.

4.1 Impedance Measurement

A two-port S-parameter approach [40] is used to calculate the input impedance of the tag antenna, which transforms the S-parameter into Z-parameters. The tag antenna is regarded as a two-port network in this approach, and the differential impedance is calculated using (3). Two semi-rigid coaxial cables and a Keysight PNA-L were required to perform the S-parameter measurements.

$$Z_t = \frac{2 Z_0 (1 - S_{11} S_{22}) + (S_{12} S_{21}) - S_{12} - S_{21}}{(1 - S_{11})(1 - S_{22}) - S_{12} S_{21}} \quad (3)$$

The Vector Network Analyser (VNA) was carefully calibrated to obtain accurate S-parameters, and the effects of the semi-rigid coaxial cables were compensated using the port extension technique. The measured and simulated impedance of the proposed tag antenna with a water bottle at 866 MHz and 915 MHz are listed in Table 8.

Table 8 Measured and Simulated impedance of the proposed tag antenna.

Frequency (MHz)	Measured	Simulated
866	$23.17 + j137.03\,\Omega$	$36.44 + j154.8\,\Omega$
915	$20.5 + j136.07\,\Omega$	$13.26 + j158.79\,\Omega$
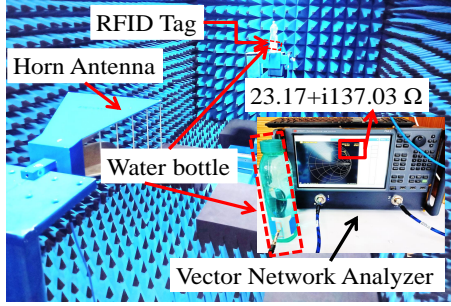
Fig. 14: Measurement setup of the proposed tag antenna with water bottle.

The theoretical chip impedance $35.58 - j154.31\,\Omega$ at 866 MHz and $32.28 - j146.83\,\Omega$ at 915MHz, is also provided for reference. The simulated and measured findings indicate similar trends, however, certain inconsistencies between the simulated and measured results were due to the manufacturing tolerances and some variation in water and HDPE bottle properties, which led to a slight deviation of the measured input impedance of the fabricated tag antenna from simulations.

4.2 Radiation Pattern Measurement

The radiation patterns of the proposed tag antenna (with water bottle) were measured in an anechoic chamber, Fig. 14, and the results shown in Fig. 15.

The bidirectional patterns, more apparent at 866 MHz, are perceived as positive for bottling lines applications where a reduction of the mutual coupling [38] among tagged water bottles in closely stacked or piled packing is expected in the bottled water industry. The maximum measured gain of the proposed tag antenna (with water bottle) was 0.05 dBi and -0.6 dBi at 866 MHz and 915 MHz, respectively. Although the proposed tag antenna was specifically designed for the 866 MHz band, results are shown additionally at 915 MHz to demonstrate its performance in the FCC band. Further, the reading range of the proposed tag antenna measured at various angles ($0°$ to $360°$) was evaluated and is presented in Fig. 16. The simulated result is also included in the figure and show reasonable agreement between both, Fig. 16 (a) and (b). Because the read range patterns are more bidirectional like, this is attractive for water inventory in industrial applications such as a conveyor belt and stockpiling where mutual coupling minimal effect ($0°$ and $180°$) is preferred.

4.3 Performance Comparison

Table 9 includes various state-of-the-art designs widely available in the literature for comparison, showing the proposed tag antenna (affixed to a water bottle), a longer read range, and a smaller footprint (miniature design) compared to other designs. For instance, although [23] is only $4 \times 7 \times 0.1$ mm bigger than the proposed counterpart, it offers a 6.68m lowered read range. Furthermore, a multi-slot tag antenna with a $36 \times 19 \times 0.7$ mm bigger size and a
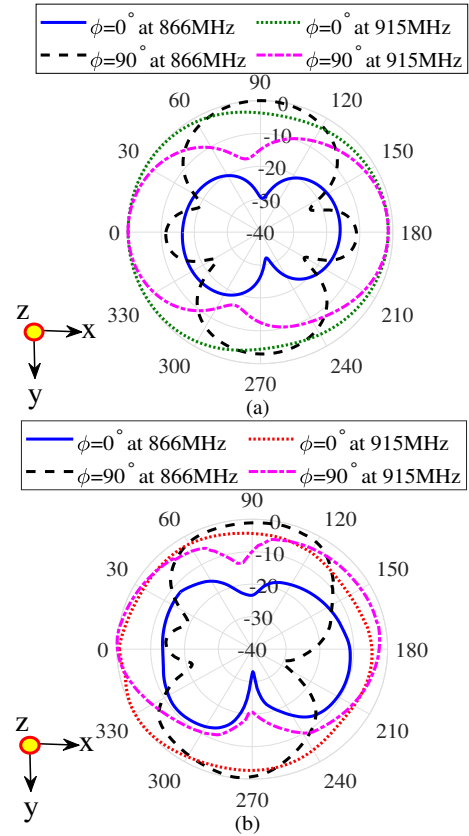
Fig. 15: (a) Simulated and (b) measured radiation patterns of the proposed tag on water-filled HDPE bottle.
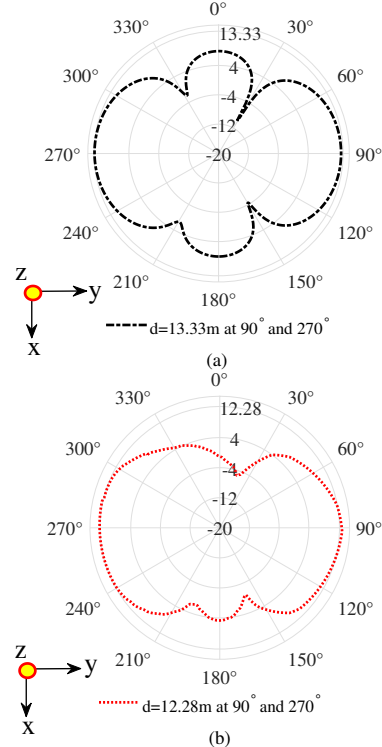
Fig. 16: (a) Simulated and (b) measured read range patterns of the proposed tag on water-filled HDPE bottle.

2.28m lower reading range was proposed in [22]. Similarly, [34] offers a lowered 4.78m read range and $75 \times 27 \times 0.4$mm bigger size. This corroborates the out performance of the proposed tag antenna in terms of compact size and long read range.

Table 9 Comparison with state-of-the-art designs.

Reference	Substrate	Size (mm)	Measured Read range (m) at 866MHz	Flexible	Miniature	Long-range (≥4m)
[7]	Polyester	86×22.5×0.05	2.2	Yes	No	No
[8]	FR4	81×23×1.5	2.5	No	No	No
[9]	Paper	40×20×0.02	~0.34	Yes	Yes	No
[13]	Rogers Ultralam 3850HT	28×13×0.35	2.51	Yes	Yes	No
[22]	F4B-2	76×32×0.8	10	No	No	Yes
[23]	polyimide	44×20×0.2	1.45-5.6	Yes	Yes	Yes
[32]	Polyester	87.8×57.9×0.05	4.25	Yes	No	Yes
[34]	FR4	115×40×0.5	7.5	No	No	Yes
[36]	Silicon	70×30×3	1.9-2.5	Yes	No	No
[41]	Plastic	87.8×57.9×0.125	4	Yes	No	Yes
This work	Polyester	40×13×0.1	12.28	Yes	Yes	Yes

5 Conclusion

This paper presents a compact, flexible, mutual coupling insensitive UHF RFID impedance transformer balun-like integrated tag antenna for long-range water bottle detection. The tag antenna comprised folded, unbalanced strips made of balun-like arms wrapped around the tag's body. The proposed tag showed good impedance matching between the antenna and the chip and an outstanding read range compared to other state-of-the-art designs, bringing a compact tag with a long detection range in liquid inventory RFID applications. The tag was found to be $12 - 50\%$ smaller in size with a > 5.83 m longer read range compared to other state-of-the-art.

6 Acknowledgments

7 References

1 Lizzi, L. and Ferrero, F., "Use of Ultra-narrow Band Miniature Antennas for Internet-of-Things Applications," *Electronics Letters*, 2015, **51**, 1964-1966.

2 Kumar, M, Sharma, A, Garcia Zuazola, IJ., "All-in-One UHF RFID Tag Antenna for Retail Garments Using Nonuniform Meandered Lines," *Progress In Electromagnetics Research Letters*, 2020 **Vol. 94**, 133-139.

3 Sharma, B. and Koundal, D., "Cattle Health Monitoring System using Wireless Sensor Network: a survey from innovation perspective," *IET Wireless Sensor System*, 2018, **8**, 143-151.

4 Svanda, M. and Polivka, M. (2016), "On-body Semi-Electrically Small tag Antenna for Ultra High Frequency Radio Frequency Identification Platform Tolerant Applications," *IET Microwave Antennas Propagation*, **10**, 631-637.

5 Abdelrahim, W. and Feng, Q. (2019), "Compact Broadband Dual-band Circularly Polarised Antenna for Universal UHF RFID Handheld Reader and GPS Applications." *IET Microwave Antennas Propagation*, **13**, 1664-1670.

6 Kumar, M, Sharma, A, Garcia Zuazola, IJ., "Bendable Ultra-High Frequency Radio-Frequency Identification Tag Antenna for Retail Garments using Nonuniform Meandered lines," *Engineering Reports* 2021; 3:e12420.

7 A. P. Sohrab, Y. Huang, M. Hussein, M. Kod and P. Carter, "A UHF RFID Tag With Improved Performance on Liquid Bottles," *IEEE Antennas and Wireless Propagation Letters*, **vol. 15**, pp. 1673-1676, 2016.

8 A. Dubok and A. B. Smolders, "Miniaturization of Robust UHF RFID Antennas for Use on Perishable Goods and Human Bodies," *IEEE Antennas and Wireless Propagation Letters*, **vol. 13**, pp. 1321-1324, 2014.

9 Quiroz, R., Alves, T., Poussot, B. and Laheurte, J.-M., "Combined RFID tag antenna for recipients containing liquids," *Electronics Letters*, **49**, 240-242, 2013.

10 Ziai, mohamad ali and Batchelor, John., "Thin ultra high-frequency platform insensitive radio frequency identification tags," *IET Microwave Antennas Propagation*, **4**, 390 - 398, 2010.

11 J. Xi and T. T. Ye, "Conformal UHF RFID tag antenna mountable on winebottle neck," *Proceedings of the 2012 IEEE International Symposium on Antennas and Propagation*, pp. 1-2, 2012.

12 S. R. Aroor and D. D. Deavours, "Evaluation of the State of Passive UHF RFID: An Experimental Approach," *IEEE Systems Journal*, **vol. 1**, no. 2, pp. 168-176, Dec. 2007.

13 D. Carlos, P. Morales, O. Diogo, S., Elson, S., Weber, "Ultra slim and small UHF RFID tag design for mounting on curved surfaces," *AEU International Journal of Electronics and Communications*, **Vol. 128**, 2021, 153502, ISSN 1434-8411.

14 R. Gonçalves, N. B. Carvalho, R. Magueta, A. Duarte and P. Pinho, "UHF RFID tag antenna for bottle labeling," *2014 IEEE Antennas and Propagation Society International Symposium (APSURSI)*, 2014, pp. 1520-1521.

15 R. Gonçalves et al., "RFID tags on cork stoppers for bottle identification," *2014 IEEE MTT-S International Microwave Symposium (IMS2014)*, 2014, pp. 1-4.

16 R. Gonçalves, R. Magueta, P. Pinho and N. B. Carvalho, "RFID passive tag antenna for cork bottle stopper," *2014 IEEE Antennas and Propagation Society International Symposium (APSURSI)*, 2014, pp. 1518-1519.

17 Kim, Y. (2013), "Design of near omnidirectional UHF RFID tag with one-off seal function for liquid bottles," *Microwave Optical Technology Letter*, 55: 375-379.

18 M. C. Caccami and G. Marrocco, "Electromagnetic Modeling of Self-Tuning RFID Sensor Antennas in Linear and Nonlinear Regimes," *IEEE Transactions on Antennas and Propagation*, **vol. 66**, no. 6, pp. 2779-2787, June 2018.

19 L. J. Görtschacher and J. Grosinger, "UHF RFID Sensor System Using Tag Signal Patterns: Prototype System," *IEEE Antennas and Wireless Propagation Letters*, **vol. 18**, no. 10, pp. 2209-2213, Oct. 2019.

20 A. Sharif, J. Ouyang, Y. Yan, A. Raza, M. A. Imran and Q. H. Abbasi, "Low-Cost Inkjet-Printed RFID Tag Antenna Design for Remote Healthcare Applications," *IEEE Journal of Electromagnetics, RF and Microwaves in Medicine and Biology*, **vol. 3**, no. 4, pp. 261-268, Dec. 2019.

21 D. Kim and J. Yeo, "Low-Profile RFID Tag Antenna Using Compact AMC Substrate for Metallic Objects," *IEEE Antennas and Wireless Propagation Letters*, **vol. 7**, pp. 718-720, 2008.

22 Tang, T., She, Y., Deng, X. and Wen, G, "Design and Radiation Mechanism Analysis of a Multi-usage Ultra-High Frequency Radio Frequency Identification tag Antenna," *IET Microwave Antennas Propagation*, **13**, 1989-1996,2019.

23 Sailing He, Yiming Zhang, Laijun Li, Yuefeng Lu, Yuan Zhang, and Hui Liu, "High Performance UHF RFID Tag Antennas on Liquid-Filled Bottles," *Progress In Electromagnetics Research*, **Vol. 165**, 83-92, 2019.

24 J. Ouyang, A. Sharif, Y. Yan and Q. H. Abbasi, "Small Conformal UHF RFID Tag Antenna for Labelling Fruits," *2019 IEEE Asia-Pacific Microwave Conference (APMC)*, 2019, pp. 33-35.

25 L. Li and W. He, "Anti-Water UHF RFID Tag Antenna with Multi-Loop Structure for Impedance Matching," *2018 Progress in Electromagnetics Research Symposium (PIERS-Toyama)*, 2018, pp. 1805-1808.

26 A. Sharif, J. Ouyang, Y. Yan, R. Long and A. Raza, "Low cost Conformal UHF RFID Tag Antenna for Plastic Water Bottles," *2018 IEEE International Symposium on Antennas and Propagation & USNC/URSI National Radio Science Meeting*, 2018, pp. 693-694.

27 Sharif, A, Ouyang, J, Raza, A, Imran, MA, Abbasi, QH,"Inkjet printed UHF RFID tag based system for salinity and sugar detection,"*Microwave Optical Technology Letter*, 2019; 61: 2161– 2168.

28 D.-B. Lin, I-T. Tang & C.-C. Wang,"UHF RFID H-Shaped Tag Antenna using Microstrip Feed Design on Metallic Objects," *Journal of Electromagnetic Waves and Applications*, 25:13, 1828-1839.

29 Y. Amin, Q. Chen, H. Tenhunen, and L. Zheng, "Performance-Optimized Quadrate Bowtie RFID Antennas for Cost-Effective and Eco-Friendly Industrial Applications," *Progress In Electromagnetics Research*, **Vol. 126**, 49-64, 2012.

30 B. Aslam, M. Kashif, MA. Azam, Y. Amin, J. Loo, H. Tenhunen,"A low profile miniature RFID tag antenna dedicated to IoT applications," *Electromagnetics*, 39:6, 393-406.

31 A. G. Santiago, C. A. Fernandes and J. R. Costa, "Broadband UHF RFID passive tag antenna for near-body operation," *2012 IEEE International Conference on RFID-Technologies and Applications (RFID-TA)*, 2012, pp. 271-274.

32 T. Bjorninen, A. Z. Elsherbeni and L. Ukkonen, "Low-Profile Conformal UHF RFID Tag Antenna for Integration With Water Bottles," *IEEE Antennas and Wireless Propagation Letters*, **vol. 10**, pp. 1147-1150, 2011.

33 A. Zaric, C. C. Cruz, A. M. de Matos, M. R. da Silva, J. R. Costa and C. A. Fernandes, "RFID-based Smart Blood Stock System [Education Column]," *IEEE Antennas and Propagation Magazine*, **vol. 57**, no. 2, pp. 54-65, April 2015.

34 Alonso, Daniel and Zhang, Qianyun and Gao, Yue and Valderas, Daniel, "UHF passive RFID-based sensor-less system to detect humidity for irrigation monitoring," *Microwave and Optical Technology Letters*, **vol. 59**, pp. 1709-1715, 2017.

35 Ting, S.-H and Wu, C.-K and Luo, C.-H, "Design of Dual Mode RFID Antenna for Inventory Management and IV Fluid Level Warning System," *International Journal of Antennas and Propagation*, **vol. 4**, 2017.

36 Q. Liu, H. Li and Y. -F. Yu, "A Versatile Flexible UHF RFID Tag for Glass Bottle Labelling in Self-Service Stores," *IEEE Access*, **vol. 6**, pp. 59065-59073, 2018.

37 A. G. Santiago and J. R. Costa and C. A. Fernandes, "Broadband UHF RFID Passive Tag Antenna for Near-Body Applications," *IEEE Antennas and Wireless Propagation Letters*, **vol. 12**, pp. 136-139, 2013.

38 Li, Mengyuan and Niu, Zhenyi and Wang, Yanhua, "An Electrically Small Antenna with a Bidirectional Radiation Pattern for UHF RFID Tags," *2018 International Conference on Microwave and Millimeter Wave Technology (ICMMT)*, pp. 1-3,

2018.

39 Sharif, A., Kumar, R., Ouyang, J. et al., "Making Assembly Line in Supply Chain Robust and Secure using UHF RFID," *Science Reports* **11**, 18041 (2021).

40 X. Qing, C. K. Goh and Z. N. Chen, "Impedance Characterization of RFID Tag Antennas and Application in Tag Co-Design," *IEEE Transactions on Microwave Theory and Techniques*, **vol. 57**, no. 5, pp. 1268-1274, May 2009.

41 T. Björninen, L. Ukkonen, L. Sydänheimo and A. Z. Elsherbeni, "Development of a low profile conformal UHF RFID tag antenna for identification of water bottles," *2011 IEEE International Symposium on Antennas and Propagation (APSURSI)*, pp. 533-536, 2011.